

Article

A Motion-Based Conceptual Space Model to Support 3D Evacuation Simulation in Indoor Environments

Ruihang Xie , Sisi Zlatanova * , Jinwoo (Brian) Lee  and Mitko Aleksandrov 

Faculty of Arts, Design and Architecture, School of Built Environment, The University of New South Wales, Sydney, NSW 2052, Australia; ruihang.xie@unsw.edu.au (R.X.); brian.j.lee@unsw.edu.au (J.L.); mitko.aleksandrov@unsw.edu.au (M.A.)

* Correspondence: s.zlatanova@unsw.edu.au

Abstract: Three-dimensional (3D) indoor models are a crucial component to simulate pedestrian evacuations realistically in indoor environments. However, existing 3D indoor models cannot fully represent realistic indoor environments to enable the simulation of 3D pedestrian motions in evacuations because spaces above/below some physical components (e.g., desks, chairs) have been largely overlooked. Thus, this paper introduces a conceptual space model to advance a space identification and classification scheme that can fully capture 3D pedestrian motions. This paper first proposes the definition and parameterisation of different 3D pedestrian motions. Then, the definition and specifications of three categories of space components are elaborated on based on the motions. Finally, a voxel-based approach is introduced to identify and classify the space components, which are demonstrated by an illustrative example. This work contributes to advancing 3D indoor modelling to enable a more realistic simulation of 3D pedestrian motions.

Keywords: 3D model; evacuation movement; pedestrian shape; space subdivision; voxel; BIM



Citation: Xie, R.; Zlatanova, S.; Lee, J.; Aleksandrov, M. A Motion-Based Conceptual Space Model to Support 3D Evacuation Simulation in Indoor Environments. *ISPRS Int. J. Geo-Inf.* **2023**, *12*, 494. <https://doi.org/10.3390/ijgi12120494>

Academic Editors: Hartwig H. Hochmair and Wolfgang Kainz

Received: 26 October 2023
Revised: 4 December 2023
Accepted: 6 December 2023
Published: 8 December 2023



Copyright: © 2023 by the authors. Licensee MDPI, Basel, Switzerland. This article is an open access article distributed under the terms and conditions of the Creative Commons Attribution (CC BY) license (<https://creativecommons.org/licenses/by/4.0/>).

1. Introduction

Pedestrian evacuations in indoor environments have gained growing traction within the past decades, such as in high-rise buildings, underground facilities, railway stations, etc., because emergency events and disasters (e.g., terrorist attacks, earthquakes, fires, gas leaks) occurring in indoor environments may readily cause severe casualties. To address these risks, evacuation simulation models are used to investigate the safety conditions of indoor environments for improving architectural design and preparing emergency management plans and strategies.

Two types of evacuation simulation models—2D/2.5D and 3D—can be recognised based on the spatial dimensions considered in evacuation modelling [1]. In 2D/2.5D evacuation simulation models [2–6], two main issues are identified. Firstly, pedestrians' motions are simplified into only walking upright and interacting horizontally with others as moving objects in 2D horizontal plans (e.g., floor slabs) or 2.5D sloped surfaces (e.g., stairs, escalators). Crucial 3D pedestrian motions (e.g., crawling, jumping) are not considered. Secondly, 3D indoor environments are inadequately represented, such as the height of indoor features (furniture or equipment) or lowered ceilings and inclined walls, which require different motion modes, such as climbing and crawling. In many emergency evacuation scenarios, 2D/2.5D evacuation simulation models may appear insufficient.

In contrast, 3D evacuation simulation models describe pedestrian evacuations based on 3D space and replicate critical 3D pedestrian motions, such as low crawling and jumping. For instance, some researchers developed social force models to simulate leaping over movable objects (e.g., chairs, boxes) [7], crawling below the smoke and fire [8] and climbing up/down automatic ticket machines [9]. Delcea et al. [10] developed an agent-based model to simulate pedestrians jumping over chairs that fall on the aisle. In fact, pedestrians inevitably opt to use 3D motions, such as crawling below or jumping up/down desks, to

avoid imminent threats like fires, earthquakes or terrorists or to facilitate a faster escape under emergency evacuations. For instance, a surveillance video of a university library in China explicitly demonstrates that some students climbed up/down automatic ticket machines during a post-earthquake evacuation [9].

However, almost all 3D indoor models that support 3D evacuation simulation are not readily adequate [1]. In most models, spaces above/below some physical components (e.g., tables, chairs, fence) in the 3D space, which are navigable for pedestrians, are not fully identified and extracted. This brings up two major challenges. Firstly, the manner in which various physical components can enable different 3D pedestrian motions and the way pedestrians move through these physical components are insufficiently investigated and modelled [1], which restricts the possible evacuation paths. Secondly, the total evacuation path length in these simulation models does not consider the extra path lengths and effort of the vertical movement (up/down) [1,11], leading to unrealistic evacuation time computation. The length of an evacuation path determines the results of the evacuation time, which is one of the most critical evaluation factors for evacuations. To address these shortcomings, spaces above/below some physical components should be distinguished thoroughly and linked to appropriate 3D pedestrian motions.

To date, 3D voxel models have been used to model spaces for indoor evacuation and navigation. For instance, Gorte et al. [12] demonstrated that 3D voxel models are a solid foundation for studying various aspects of evacuation modelling. Several studies [13–16] discretised stairs into uniform voxels to extract a 3D surface for an evacuation simulation. Bandi and Thalmann [17] decomposed 3D indoor models into voxels and generated an optimal path for pedestrians based on the voxels on the upper surface of objects. Two studies [18,19] also used 3D voxel models as the basis of indoor path planning approaches for drones. Moreover, several studies [20–23] used the octree structure to decompose indoor environments for indoor navigation. In short, using 3D voxel models could be an appropriate way to extract spaces above/below physical components since it is convenient and effective to digitally describe indoor spaces if a suitable voxel resolution is applied. This representation can readily provide the height information of indoor spaces and enable computing paths above, below or around physical components [1,24].

Thus, this paper introduces a conceptual space model to provide a more precise space definition and classification scheme that fully considers 3D space to support more typical pedestrian motions in evacuations. Firstly, the definition and parameterisation of different 3D pedestrian motions are introduced. Subsequently, three categories of space components considering the motions are conceptualised and characterised to design the conceptual space model. Finally, a voxel-based approach is introduced to identify and classify space components. The contributions of our paper are threefold: (1) introducing the definitions and parameterisation of 3D pedestrian motions, which helps to recognise and classify space components; (2) defining three categories of space components, which can enhance the composition and specifications of indoor spaces; (3) employing a voxel-based approach for describing the space components and elaborating their classification process, which can assist in the automatic identification and classification of indoor spaces.

The remainder of the article is organised as follows. Section 2 covers related works on 3D pedestrian motions, pedestrian shapes in 3D motions and indoor space classification. Section 3 articulates assumptions, definitions and specifications related to 3D pedestrian motions and space components. Section 4 elaborates upon the procedures and demonstration of the voxel-based space identification and classification. Section 5 concludes with an analysis of the proposed model and outlines directions for future research.

2. Related Works

This section reflects related background information, similar research and promising concepts for 3D pedestrian motions, pedestrian shapes in 3D motions and indoor space classification.

2.1. Three-Dimensional Pedestrian Motions

Under normal circumstances, pedestrians primarily walk upright. This type of motion can become difficult and potentially hazardous during some emergency situations, where congestion, smoke and low visibility can cause pedestrians to trip, stumble or compete with others. Thus, pedestrians also adopt alternative motions for a quicker escape. A recent study [11] categorised the 3D interaction between pedestrians and indoor environments into five types: stepping over, crawling, bent-over walking, jumping over and climbing over. While the study highlighted the prevalence of the interaction in actual evacuations, it lacked detailed definitions and specifications of each motion.

To investigate 3D pedestrian motions, researchers carried out a series of experiments. Notably, low crawling and knee and hand crawling were extensively investigated in evacuation experiments [8,25–32]. The two motions are often adopted by pedestrians to evacuate from life-threatening emergencies, such as fires, earthquakes or shootings, significantly reducing pedestrian speed and requiring more physical effort. For example, a study [8] performed two evacuation experiments about knee and hand crawling and walking upright and found lower crawling density near the exit compared to walking density.

Bent-over walking is another motion observed in indoor environments with constrained vertical spaces that compel pedestrians to bend their bodies to walk under falling or hanging ceilings. For instance, a study [33] investigated different pedestrian motions with varying available heights and extracted bent-over walking trajectories to analyse speed–density relationships. Additionally, a study [34] conducted a series of evacuation experiments that compared three situations of obstacles: obstacles absence, obstacles that pedestrians can choose to pass by or step over and obstacles that pedestrians can only pass by. Another study [10] also experimented with evacuation from a classical and collaborative classroom. The authors observed that the falling chairs on the aisle that completely blocked the aisle made students jump over it during evacuation.

In summary, 3D pedestrian motions are commonly observed in real evacuations and have garnered attention from researchers. However, the classification, definition and specifications of these 3D pedestrian motions have not been found in the reviewed studies.

2.2. Pedestrian Shapes in 3D Motions

Different pedestrian motions require distinct postures, leading to variations in the shapes of pedestrians. Pedestrian shapes in 3D motions can be classified into two types: 2D and 3D shapes.

The 2D shape of a walking upright person is represented by a three-circle shape [35], ellipse [36–38], circle [7,39], spheropolygon [40,41] or spherocylinder [42,43]. A pedestrian's shoulder width and chest thickness are the two main factors to be specified in these representations. Other studies use a 2D grid's cell to represent a space occupied by a pedestrian walking upright. The shape of the cell can be a square [44] or hexagon [45]. Furthermore, some studies abstracted certain 3D pedestrian motions into 2D shapes. For example, a study [8] assumed that the 2D shape of knee and hand crawling is two-circle shaped, excluding the leg part. In comparison, another study [27] used two 0.4 m × 0.4 m square cells to represent a space for knee and hand crawling. Similarly, a study [46] assumed that bent-over walking and knee and hand crawling occupy two square cells.

Additionally, some studies [47–49] using Pathfinder (2021.04) or Unity software adopted the 3D shape of walking upright for collision avoidance from physical components and other pedestrians. The two types of software [50,51] use a cylinder to represent the 3D shape of a pedestrian walking upright, with the diameter and height as two main specified factors. The diameter is used for collision testing and path planning, representing the shoulder width of a pedestrian, while the height is used to limit overhead collisions, specifying the height of a pedestrian. Nevertheless, the 3D shapes of other pedestrian motions are insufficiently addressed in existing studies.

Currently, evacuation simulation researchers commonly employ 2D shapes to model pedestrian behaviours and patterns in evacuation simulations. For instance, a spherocylindrical shape allows for more realistic competitive behaviour descriptions than a simple 2D circle shape [52]. In these studies, the areas available for pedestrian motions have typically been extracted solely from floor slabs, stairs and ramps, so the focus lies on modelling behavioural mechanisms and patterns based on the 2D shapes of pedestrians. However, to obtain spaces above/below physical components for 3D evacuation simulations, pedestrians should not be regarded as 2D shapes but as 3D objects. As discussed above, different 3D pedestrian motions vary in size and height, consequently imposing certain indoor space requirements. For example, the clearance between a ceiling and a floor slab to allow low crawling or walking upright is different. As such, classifying the 3D pedestrian shapes with respect to different 3D pedestrian motions can enrich the 3D indoor models to support 3D evacuation simulations.

2.3. Indoor Space Classification

Currently, indoor spaces are mainly classified into navigable/non-occupied and non-navigable/occupied spaces using semantics inherited from building construction spaces (e.g., rooms, corridors, stairs) and physical components (e.g., furniture, walls, access rights). For instance, IndoorGML 1.0 [53] classifies space cells into NavigableSpace and NonNavigableSpace. By comparison, CityGML 3.0 [54] differentiates physical spaces into occupied and unoccupied spaces. Also, some studies [55–58] adopted this binary partitioning to support the classification of indoor spaces and path derivation. Interesting reviews [24,59] related to indoor spaces can also be found in studies.

Nevertheless, indoor spaces are not always sharply distinguishable. Since many spaces cannot be rigorously classified as navigable/unoccupied or non-navigable/occupied spaces, semantic models have been presented to classify indoor spaces further [60]. Moreover, several space models have also been developed. Yan et al. [61] classified the entire built environment into indoor, outdoor, semi-indoor and semi-outdoor spaces, but the focus of the study is not on indoor spaces. Notably, Diakit  and Zlatanova [62] identified and classified indoor spaces into smaller granularity, including object space (O-space), functional space (F-space) and remaining space (R-space). The O-spaces are non-navigable and occupied by semi-mobile objects, such as desks and chairs. The F-spaces, being the spaces providing access to objects, are navigable under the condition that they are used by semi-mobile objects or activities of mobile objects. The R-spaces are freely navigable and obstacle-free. One of the applications of the subdivision is from Nikoohemat et al. [63], who enabled users to automatically generate 3D indoor models from point clouds and extract indoor navigation networks. A recent study [64] subdivided a room into smaller units and presented a subspace framework to express the hierarchy of indoor spaces.

The above-discussed research is not specially designed for pedestrian evacuation simulation. It did not consider 3D motions and corresponding pedestrian shapes, which require more elaborated subdivisions of indoor spaces. Notably, a study [65] incorporated all kinds of space-related notions as prepositions for localisation. For example, “above” and “below” and similar were mentioned in the study, but they were not explicitly elaborated as space subdivisions. In short, the existing classification of indoor spaces remains at a particular granularity, which is not sufficient for evacuation simulation. There is still significant potential for exploring indoor spaces to reflect 3D pedestrian motions.

3. Assumptions, Definitions and Specifications

This section presents a novel conceptual space model to support 3D evacuation simulation. Two fundamental assumptions, the definitions and specifications related to different 3D pedestrian motions and space components, are articulated.

3.1. Fundamental Assumptions

The conceptual model is built on two fundamental assumptions related to the shape and size of a pedestrian and referential expressions between a pedestrian and a physical component as follows:

1. We assume the standard shape and average size of a pedestrian. This study only considers an individual rather than a group of pedestrians. Also, we assume that a pedestrian carries no bag or luggage. Moreover, we exclude wheeled motions (e.g., wheelchairs, scooters, trolleys). The walking mode is most widely used in indoor spaces as a consensus in the evacuation domain to simulate pedestrian evacuation.
2. Referential expressions from a first-person perspective are utilised to describe the placement of a pedestrian and a physical component, providing a nuanced understanding of placements in the context of 3D evacuation simulation. The vertical relations of above and below are primarily considered in the context of the simulation, with examples such as a pedestrian crawling below a computer desk and bent-over walking above a bed.

3.2. Three-Dimensional Pedestrian Motions

3.2.1. Definitions of 3D Pedestrian Motions

We classify 3D pedestrian motions into *3D movements* and height-related *3D actions* informed by existing studies and analysis of real evacuation data. Three-dimensional movements indicate moving patterns while navigable surfaces remain the same. We introduce the following four types of 3D movements:

- *Low crawling* corresponds to dragging the body close to some physical components' surfaces (e.g., floor slabs, desks, ramps) (see Figure 1a).
- *Knee and hand crawling* refers to moving forward using hands and knees (see Figure 1b).
- *Bent-over walking* is bending the body forward and downward, sometimes simultaneously bending the knees (see Figure 1c).
- *Walking upright* means moving in full size by lifting and setting down each foot in turn, without a need to have both feet off the ground at once (see Figure 1d).

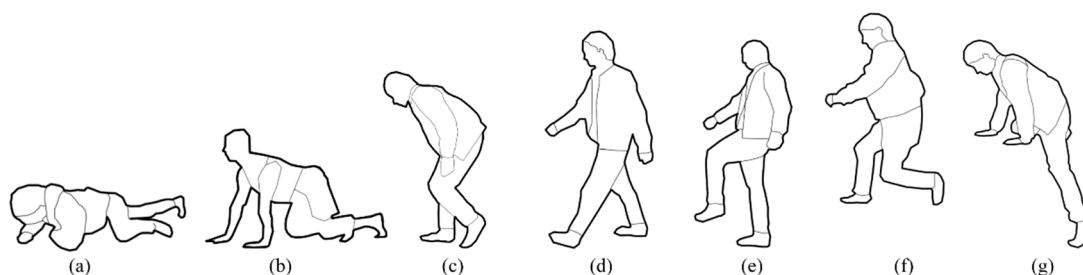


Figure 1. Schematic diagram of 3D pedestrian motions: (1) 3D movements: (a) low crawling, (b) knee and hand crawling, (c) bent-over walking and (d) walking upright; and (2) and 3D actions: (e) stepping up/down, (f) jumping up/down and (g) climbing up/down.

By comparison, height-related 3D actions refer to moving to a higher or lower position, i.e., a change in navigable surfaces is performed. We define the following six 3D actions:

- *Stepping up/down* refers to lifting and setting down one's foot or one foot after the other to move up/down a higher or lower position, never having both feet off the ground at once (see Figure 1e).
- *Jumping up/down* is pushing oneself off a surface and having both feet into the air (see Figure 1f).
- *Climbing up/down* is moving to a higher or lower position with effort, typically using both hands and feet (see Figure 1g).

3.2.2. Parameterisation of 3D Pedestrian Motions

Each 3D pedestrian motion imposes certain requirements on indoor spaces, helping to define and identify space components. Consequently, pedestrian shapes in 3D movements are specified and parameterised. Also, the thresholds of 3D actions are introduced. These parameters and thresholds are related to pedestrians only and are independent of indoor spaces.

We abstract pedestrian shapes in 3D movements into 3D cuboids. The choice to represent pedestrians using 3D cuboids rather than 3D cylinders, as used in some existing studies and applications, is primarily based on practical considerations and modelling requirements. A cuboid provides a more straightforward representation of the pedestrian's overall shape and dimensions. It is easier to define and parameterise the dimensions of a cuboid (i.e., height, width, length) than a cylinder. Moreover, cuboid calculations are generally computationally efficient, involving simple geometric operations such as intersection tests and distance calculations. In contrast, working with cylindrical shapes may require more complex mathematical operations, such as calculating distances between non-axis-aligned cylinders or detecting intersections with irregularly shaped objects.

Specifically, the four distinct movements are standardised as four types of cuboids, each characterised by specific height, length and width as follows: low crawling (h_l, l_l, w_l), knee and hand crawling (h_k, l_k, w_k), bent-over walking (h_b, l_b, w_b) and walking upright (h_u, l_u, w_u) (see Figure 2). Obviously, the cuboids' height and width should be various and necessitate different parameters to define. In most cases, the length of these cuboids remains consistent due to the uniformity of shoulder length. However, different parameters are introduced to the length of the cuboids, as they provide flexibility, enabling the users to use different lengths on some occasions. For example, when a pedestrian is low crawling or knee and hand crawling, his/her elbows may extend outwards beyond the shoulder length.

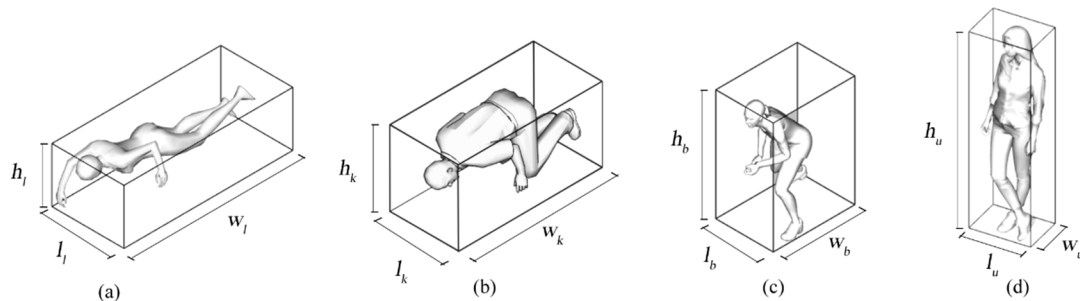


Figure 2. Three-dimensional cuboids for the four types of three-dimensional movements: (a) low crawling, (b) knee and hand crawling, (c) bent-over walking, (d) walking upright.

Three-dimensional actions are used when moving from one surface to another at different heights. To distinguish between the actions, we introduce maximum height thresholds. Different maximum height thresholds for stepping up/down, jumping up/down and climbing up/down are defined to establish the maximum heights for each of the actions, denoted as h_s , h_j and h_{cl} , respectively. The maximum height of climbing up/down is significantly greater than what can be achieved through the other two actions. Thus, the maximum height between two surfaces a pedestrian can access is determined by the threshold h_{cl} . Furthermore, treating ascending and descending actions (e.g., stepping up and stepping down, jumping up and down) as symmetric actions with the same thresholds reduces the number of parameters and thus leads to easier analysis and mathematical calculations. This symmetry does not mean that a pedestrian can only use symmetric actions to move up and down an object. A pedestrian can employ a combination of actions to move up and down an object, such as jumping up a table and then climbing down it. In summary, the values of these parameters and thresholds can be adjusted according to different pedestrian characteristics and modellers' preferences.

3.3. Space Components

3.3.1. Definition of Space Components

Following previous research, we assume that indoor spaces incorporate physical components. Physical components are composed of static objects, movable objects and dynamic objects [1] (see Figure 3a). Static objects do not move by themselves or cannot be moved (e.g., walls, stairs, columns). Movable objects do not move by themselves but can be moved by pedestrians under specific situations (e.g., chairs, stools, tables). Dynamic objects can move by themselves at variable speeds (e.g., robots, drones). Traditionally, navigable spaces for pedestrian evacuation are derived from floor slabs, stairs and ramps, which are static objects. However, many movable objects may offer an additional navigable space or reduce the navigable space if the height dimension of 3D space above the movable objects is available.

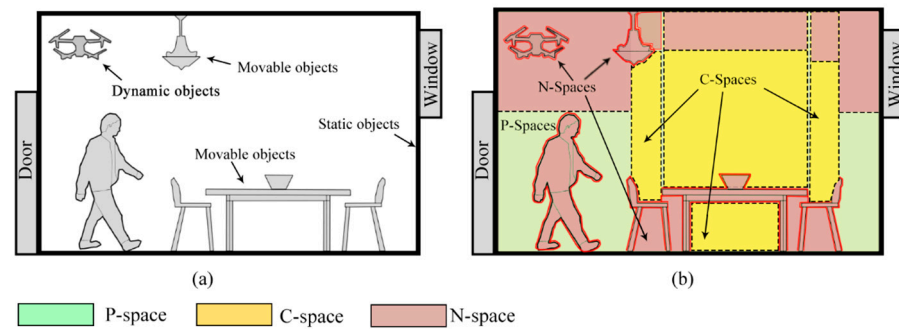


Figure 3. (a) A populated room with static, movable and dynamic objects. (b) The room with space components: P-space (green), C-space (yellow) and N-space (red).

Thus, based on the characteristics of 3D pedestrian motions and physical components, we classify indoor spaces into three types of space components, namely, freely navigable space for pedestrians (P-space), navigable space under conditions (C-space) and non-navigable space (N-space). The P-, C- and N-spaces are non-overlapping (see Figure 3b). Physical components are located in N-spaces. In our work, the whole indoor space is represented by a general variable, i.e., I-space. I-space is the union of P-spaces, C-spaces and N-spaces and is expressed as:

$$I = P \cup C \cup N \quad (1)$$

where I, P, C and N denote the indoor space, P-spaces, C-spaces and N-spaces, respectively.

The three categories of space components are defined as follows:

1. P-spaces refer to unoccupied spaces available for pedestrians to walk upright on the following static objects: floor slabs, stairs and ramps.
2. C-spaces refer to spaces above/below physical components, where pedestrians can move through using 3D movements in abnormal circumstances. C-spaces are located above the top surface of movable objects (e.g., chairs, sofas) or stationary dynamic objects (e.g., cleaning robots) that require 3D actions, or below the bottom surface of static objects (e.g., low roofs/ceilings, stairs) or movable objects (e.g., tables). According to the four types of 3D movements, the C-spaces are further classified into:
 - C_l -spaces, where pedestrians can only move through the spaces using low crawling.
 - C_k -spaces, where pedestrians can move through the spaces using knee and hand crawling.
 - C_b -spaces, where pedestrians can move through the spaces using bent-over walking.
 - C_u -spaces, where pedestrians walk upright on movable or dynamic objects to move through the spaces.
3. N-spaces refer to spaces that

- Are occupied by static, movable and dynamic objects;
- Any of the 3D movements cannot move through;
- Are unreachable through any of the 3D actions;
- Are not used for evacuation simulation.

The classification and definitions of P-, C- and N-spaces differ from those of R-, F- and O-spaces proposed in a previous study [62]. Firstly, R-spaces correspond to the remaining space after subtracting O-spaces and F-spaces, causing some overhead spaces that pedestrians cannot reach to be freely navigable. These overhead spaces are not used for evacuation simulation, bringing unnecessary computation in identifying and classifying spaces. Furthermore, F-spaces only represent spaces around objects that allow for 3D actions. C-spaces are considered part of either the R- or O-space. Consequently, spaces for different 3D movements are not distinguished, which causes difficulties in the behavioural modelling of how different physical components enable 3D movements and how pedestrians move up/down them in 3D space. Finally, O-spaces do not explicitly address some unreachable non-navigable spaces that are not used for evacuation simulation, such as overhead spaces, spaces that 3D movements cannot move through. Therefore, the classification of P-, C- and N-spaces in this study is more appropriate for supporting the simulation of 3D pedestrian motions.

Using the definitions introduced above, we give examples of P-, C- and N-spaces (see Figure 4). For instance, Figure 4g represents an N-space occupied by a chair and an N-space below the chair that any of the 3D movements cannot fit in. Figure 4h,i, respectively, illustrate an N-space above a cupboard that is unreachable to pedestrians and an overhead N-space that is not used for evacuation simulations.

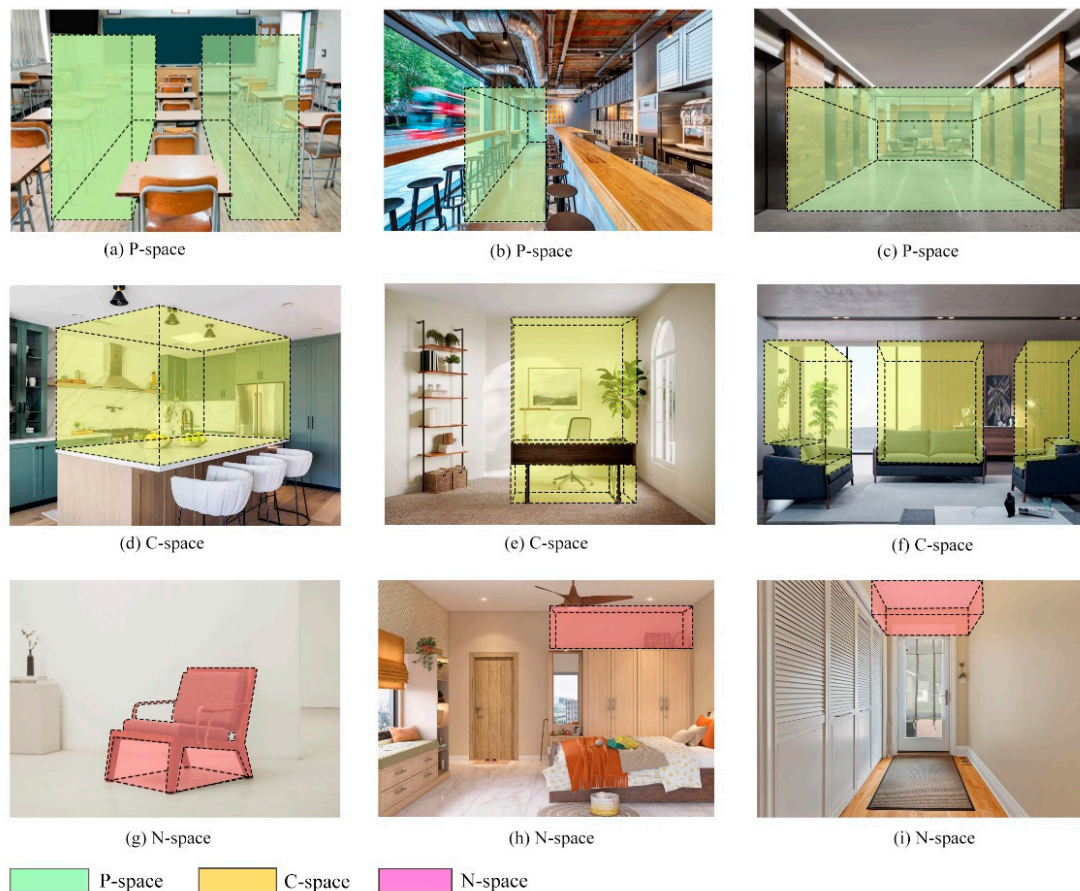


Figure 4. Spaces are categorised into three types according to the definitions of P-, C- and N-spaces.

3.3.2. Specifications of Space Components

In this subsection, we elaborate on the specifications of three space components.

1. P-spaces

To identify a P-space, two key factors must be considered: (1) the dimensions of the 3D cuboid for walking upright and (2) the semantics of the static object that pedestrians walk on. A P-space harbours a pedestrian walking upright on the top surfaces of three physical components, which are static objects only, i.e., floor slabs, stairs and ramps. The height of a P-space is theoretically up to another physical component (static and dynamic objects), such as ceilings or lamps. However, we denote the P-space height to be equal to the height of the cuboid for walking upright h_u . We assume that pedestrians cannot access overhead spaces. Therefore, the spaces are not needed with their max extension (see Figure 4a–c). The length and width of the P-space are influenced by the semantics of the static objects. The minimum length and width of a P-space must be equal to or larger than the dimensions (l_u and w_u) of the cuboid for walking upright for floor slabs and ramps. Staircases are an exception. If a staircase is provided with treads and the width of the tread is smaller than w_u , the space above the step is still classified as a P-space.

2. C-spaces

As presented above, C-spaces are classified into four types based on the four 3D movements (see Figure 5). To identify a C-space, three key factors are crucial: (1) the semantics of the physical component that defines navigable surfaces for 3D movements, (2) the dimensions of 3D cuboids and (3) the maximum height threshold of climbing up/down.

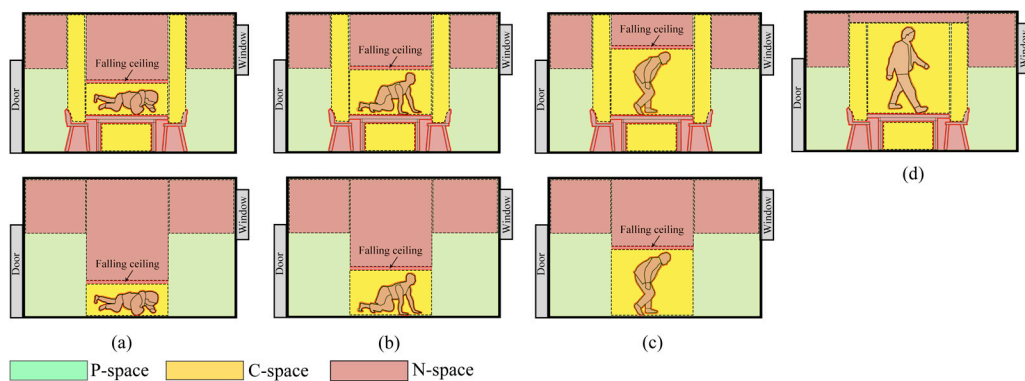


Figure 5. Four types of C-spaces. (a) C_1 -spaces. (b) C_k -spaces. (c) C_b -spaces. (d) C_u -spaces.

- **Semantics of physical component:** If the semantics of physical components indicate movable or dynamic objects, C-spaces are above them. If the semantics refers to the floor slabs, stairs and ramps of static objects, but the surface where pedestrians move on remains the same, C-spaces are below static or movable objects. A typical example is a movable object “table”. C-spaces can be identified both above and below the table.
- **Dimension of 3D cuboids:** A space is identified as a C-space only when it accommodates an entire cuboid, i.e., considering height, length and width. This rule has one exception: spaces below static or movable objects can be classified into C-spaces if (1) the height and length of the cuboids for bend walking, knee crawling and low crawling can be fit within the space and (2) adjacent spaces (P-spaces or C-spaces) can accommodate a portion of their width. A table is a good illustration of this exception (see Figure 6). Additionally, the height of a C-space corresponds to that of the cuboid it accommodates. The horizontal size and shape of a C-space above a movable or dynamic object align with the dimensions of the object’s top surface. The horizontal size and shape of a C-space positioned below a static or movable object, on the other hand, match the dimensions of the object’s bottom surface. For each subtype of

C-spaces apart from C_1 -spaces, some spaces in one subtype may be used for another movement, given that the length and width of that movement can be ensured. For example, C_u -spaces can be used for bent-over walking, knee and hand crawling and low crawling if the C_u -space is large enough to allow for the lengths l_b , l_k and l_l and the widths w_b , w_k and w_l of the three movements.

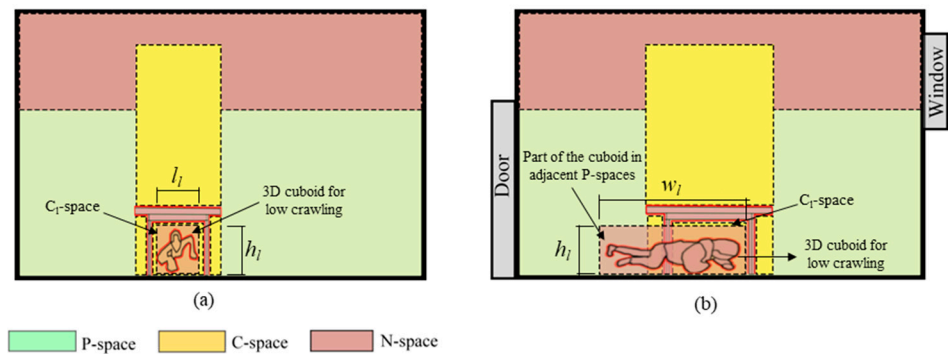


Figure 6. A C_1 -space under a table. (a) h_l and l_l of the 3D cuboid for low crawling fit within the space. (b) Adjacent P-spaces accommodate a portion of the w_l .

- Maximum height threshold of climbing up/down: To identify if a C-space above movable or dynamic objects is reachable, a parameter defines the clearance from the current to the targeted surface of movement, denoted as h_n (see Figure 7). The clearance h_n must be greater than 20 cm and less than the maximum height threshold of climbing up/down, i.e., $20\text{ cm} < h_n \leq h_{cl}$. The threshold of 20 cm is strictly specified to indicate that regular stair treads do not involve a 3D action. The maximum height threshold depends on a person's physical characteristics.

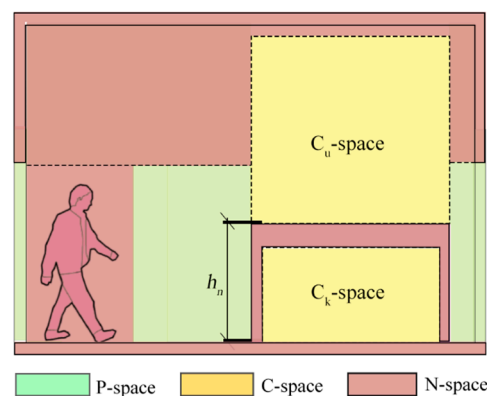


Figure 7. Schematic diagram of a parameter for the clearance h_n .

3. N-spaces

The identification and classification of N-spaces rely on P-spaces and C-spaces. Once all P-spaces and C-spaces have been identified and classified, the remaining spaces are N-spaces.

4. Demonstration of the Conceptual Space Model

In this section, we demonstrate the conceptual model by using a voxel approach. A voxel-based representation is an appropriate way to identify P-, C- and N-spaces, which allows easy measuring of heights, lengths and widths. Spaces in indoor environments possess diverse 3D shapes and sizes, which traditional vector geometric models fail to handle efficiently. Furthermore, the voxel-based representation fosters the labelling of voxels associated with space components [18,21,66].

4.1. Procedures of Space Identification and Classification

This paper concentrates on BIM models and, more specifically, Industry Foundation Classes (IFC) indoor models. IFC is a standardised format used to describe building and construction industry data. It provides a comprehensive representation of buildings, including their geometry and various semantics of building elements [67], which are useful for our space identification and classification.

Figure 8 illustrates space component identification and classification workflow.

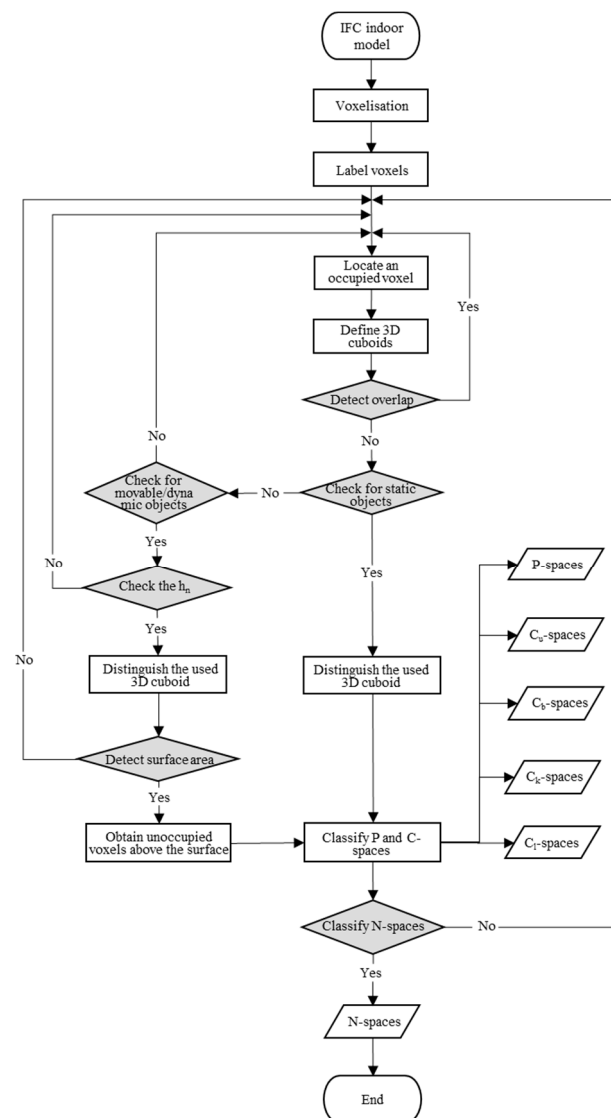


Figure 8. Flowchart of the space identification and classification based on the conceptual space model.

- **Voxelisation:** An IFC indoor model is voxelised. We enclose the IFC indoor model within a bounding box that aligns with the coordinate axes (X, Y, Z). Each voxel carries the IFC semantics about the physical components and spaces it represents.
- **Label voxels:** The voxel labels are organised based on the original IFC semantics. All voxels with the IFC semantics related to physical components (e.g., *IfcSlab*, *IfcStair*, *IfcRamp* and *IfcWalls*) are labelled as occupied voxels, while the rest of the voxels are marked as unoccupied voxels. Furthermore, some occupied voxels are marked as static object, movable object or dynamic object types. The static object only incorporates the semantic information of floor slabs, stairs and ramps.

- Locate an occupied voxel: We traverse the voxels to locate an occupied voxel. The voxel space is traversed once, voxel by voxel, from the bottom to top, left to right and front to back of the bounding box.
- Define 3D cuboids: Four types of 3D cuboids are simultaneously defined above the traversed occupied voxel. The voxel number of each 3D cuboid depends on the voxel resolution and corresponds to the lengths l_u, l_b, l_k, l_l , widths w_u, w_b, w_k, w_l and heights h_u, h_b, h_k, h_l . The occupied voxel is suggested to be right below the bottom centre of the 3D cuboids and towards the main direction of movements (see Figure 9).

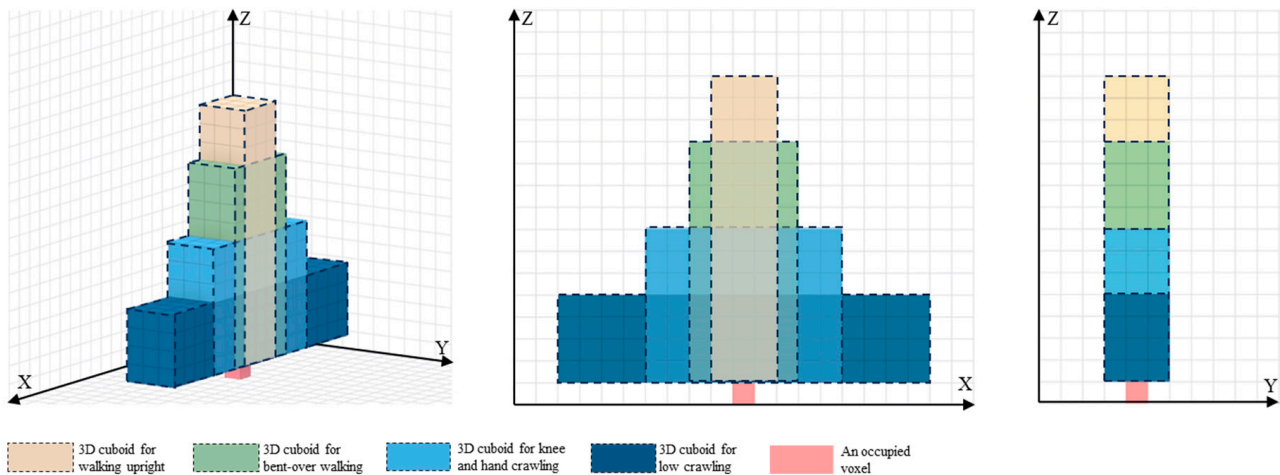


Figure 9. Location of the four 3D cuboids above an occupied voxel in the X, Y and Z dimensions.

- Detect overlap: We detect if any of the 3D cuboids overlap with physical components. If no overlap is detected, i.e., the space/voxels overlapping with the 3D cuboids are all unoccupied, they are classified into a potential P-space or C-space (to be checked in the next steps). In contrast, if the examined voxel space has occupied voxels that overlap with the 3D cuboid, the corresponding space cannot accommodate the 3D cuboids. Thus, if one or more 3D cuboids without an overlap exist, the procedures progress to the subsequent set of rules. If all the 3D cuboids overlap with physical components, the procedures go back to traverse the next occupied voxel.
- Check for static objects: The semantics associated with the traversed occupied voxel are checked. If the voxel has the semantics of a static object, the examined voxel space could potentially be P-spaces or C-spaces below static or movable objects. We proceed to recognise the used 3D cuboid in step (7). Otherwise, the space may be C-spaces above movable or dynamic objects. We proceed directly to step (8).
- Distinguish the used 3D cuboid: We distinguish the 3D cuboid without an overlap that is used for recognising and classifying space components. A classification sequence prioritises the 3D cuboid for walking upright, followed by the cuboid for bent-over walking, subsequently the one for knee and hand crawling, and lastly the cuboid for low crawling. For example, if the cuboid for walking upright does not overlap with any physical components, the unoccupied voxels within the cuboid will be assigned in the next step. Other 3D cuboids will not be used for classification. If the cuboid for walking upright experiences an overlap, the following bent-over walking cuboid is checked. The procedure continues until a 3D cuboid that does not overlap with any occupied voxel is found. The unoccupied voxels are potential P- and C-spaces and are classified in step (13).
- Check for movable/dynamic objects: When the semantics of the traversed occupied voxel are not a static object, we further check if the semantics correspond to a movable object or dynamic object. If the semantics align with either of these, we proceed to the subsequent steps. Otherwise, we begin to locate a new occupied voxel.

- Check the h_n : The clearance h_n is checked if it falls in the range of $20 \text{ cm} < h_n \leq h_{cl}$. To this end, we search unoccupied voxels within X and Y dimensions that surround and adjoin horizontally to the movable or dynamic object that the traversed occupied voxel belongs to. Afterwards, we detect whether any occupied voxels with the semantics of static object, movable object or dynamic object are situated directly below these searched unoccupied voxels within the distance range. If the occupied voxel exists, the procedures start with the next rules. If no occupied voxel is within the range, the procedures return to traverse the next occupied voxel.
- Distinguish the used 3D cuboid: This step remains consistent with step (7), which prioritises different 3D cuboids for recognising and classifying space components.
- Detect surface area: The top surface of the movable or dynamic object is checked for whether the used 3D cuboid can be placed on it. We perform a voxel search in the horizontal plane, neighbouring the currently traversed occupied voxel, within the X and Y dimensions. Then, we check if these voxels are all occupied. If yes, the cuboid can be placed on the surface, and we continue with the classification process. If not, we revert to traverse the next occupied voxel.
- Obtain unoccupied voxels above the surface: We obtain unoccupied voxels above the entire top surface of the movable or dynamic object. A horizontal search is performed to find all adjacent occupied voxels that surround the traversed occupied voxel and possess the semantics of a movable object or dynamic object. For each occupied voxel of the whole surface, a neighbouring search in the Z dimension is conducted to find unoccupied voxels. The search commences from the entire surface and terminates at a height equivalent to that of the 3D cuboid.
- Classify P- and C-spaces: According to the type of used 3D cuboid, the unoccupied voxels within the 3D cuboid or above the whole surface are added to different pre-defined 3D arrays for P-spaces, C_u -spaces, C_b -spaces, C_k -spaces or C_l -spaces. For instance, if the traversed occupied voxel's semantics is a movable object or dynamic object and the cuboid for walking upright is used, unoccupied voxels above the surfaces are assigned into 3D arrays for C_u -spaces. Each unoccupied voxel can only be added to a 3D array. We exclude the duplicates from within the array. After classifying the unoccupied voxels, this classification associated with the traversed occupied voxel finishes.
- Classify N-spaces: We check if all the occupied voxels are traversed. If all the occupied voxels have been traversed, all occupied voxels and the rest of the unoccupied voxels that are not classified as P-spaces and C-spaces are categorised into N-spaces. The whole procedure is then finished. If not, the procedures revert to locate another occupied voxel.

Overall, using the procedures, the identification and classification of space components can be completed conveniently and efficiently.

4.2. Demonstrating the Model for a Room of a Building

The conceptual space model presented above is illustrated for one room. An IFC indoor model of the Genesis 1560 Trapelo, a three-story office and laboratory building in Waltham, MA, USA (<http://openifcmodel.cs.auckland.ac.nz/>, accessed on 9 January 2022) was used as it had a variety of physical components. For the sake of clarity, the IFC model was simplified prior to voxelisation. Figure 10 illustrates the room, which consists of 79 chairs, 10 round tables, 3 tables, 1 wardrobe, 3 sofas, 15 desks and aisles accessible for pedestrians. Furthermore, the physical parts of doors and windows are removed from the room.

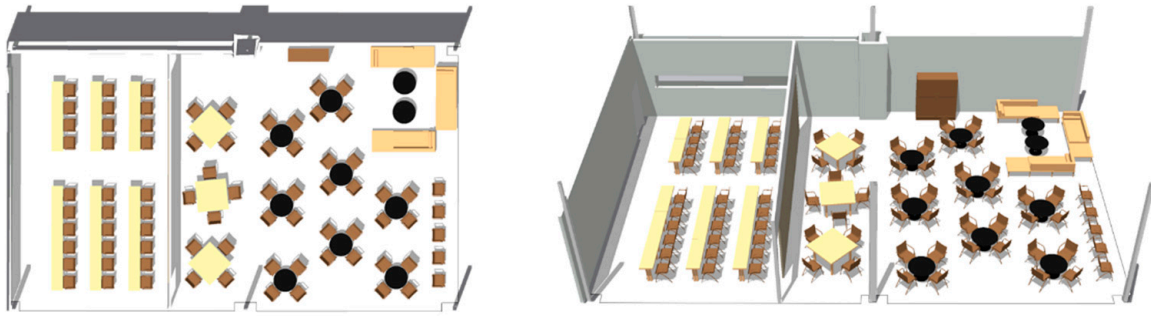


Figure 10. BIM IFC model of a furnished room.

First, the sizes of 3D cuboids were configured (Table 1). The maximum height of climbing up/down h_{cl} of an ordinary pedestrian is configured at 110 cm. For this demonstration, an average person is considered, but it is possible to consider the dimensions of male, female, child or elderly and define dedicated space subdivisions.

Table 1. Size of 3D cuboids for an ordinary pedestrian.

Size of 3D Cuboids (cm)	Height	Length	Width
Walking upright	170 (h_u)	30 (l_u)	30 (w_u)
Bent-over walking	140 (h_b)	30 (l_b)	70 (w_b)
Knee and hand crawling	90 (h_k)	30 (l_k)	110 (w_k)
Low crawling	40 (h_l)	30 (l_l)	170 (w_l)

Subsequently, we voxelised the 3D indoor model using the Unity 3D Engine. We experimented with a range of voxel resolutions in a range of 1 cm to 10 cm. After multiple tests, we used a 10 cm voxel resolution for the model. This size allowed computations to be performed in less than 1–2 min, still providing a sufficiently higher level of accuracy for objects' geometry. Considering the semantic information of physical components, we manually use the sizes of cuboids to analyse whether/which cuboids can fit in a voxelised space and whether the clearance h_n falls in the 110 cm.

Figure 11 illustrates the identification and classification process of C-spaces above/below the movable objects in the room. Examples of these movable objects on floor slabs include a chair, a round table, a desk, a sofa and a wardrobe, exhibiting irregular shapes and various sizes. To begin, the meshes of these movable objects are voxelised to be occupied voxels that directly correspond to N-spaces. Subsequently, we identify the semantics of these objects. Then, we check how many voxels are above and below the objects to identify whether the sizes of the cuboids can fit in the spaces. It can be observed in Figure 11 that, except for the space below the sofa, other spaces can accommodate the cuboids for walking upright, low crawling or knee and hand crawling. For instance, the space above the chair is used for waking upright, while the space below the desk accommodates knee and hand crawling. However, the backrest of the sofa cannot accommodate the whole cuboid for walking upright, so the space above the backrest is an N-space. Then, these spaces are checked to see if they are accessible to pedestrians to move up/down, i.e., the clearance h_n . The results show that the space above the wardrobe is inaccessible to pedestrians and is thus classified as an N-space. Finally, we obtain entire spaces/unoccupied voxels and classify them into different types of C-spaces according to the cuboid they accommodate.

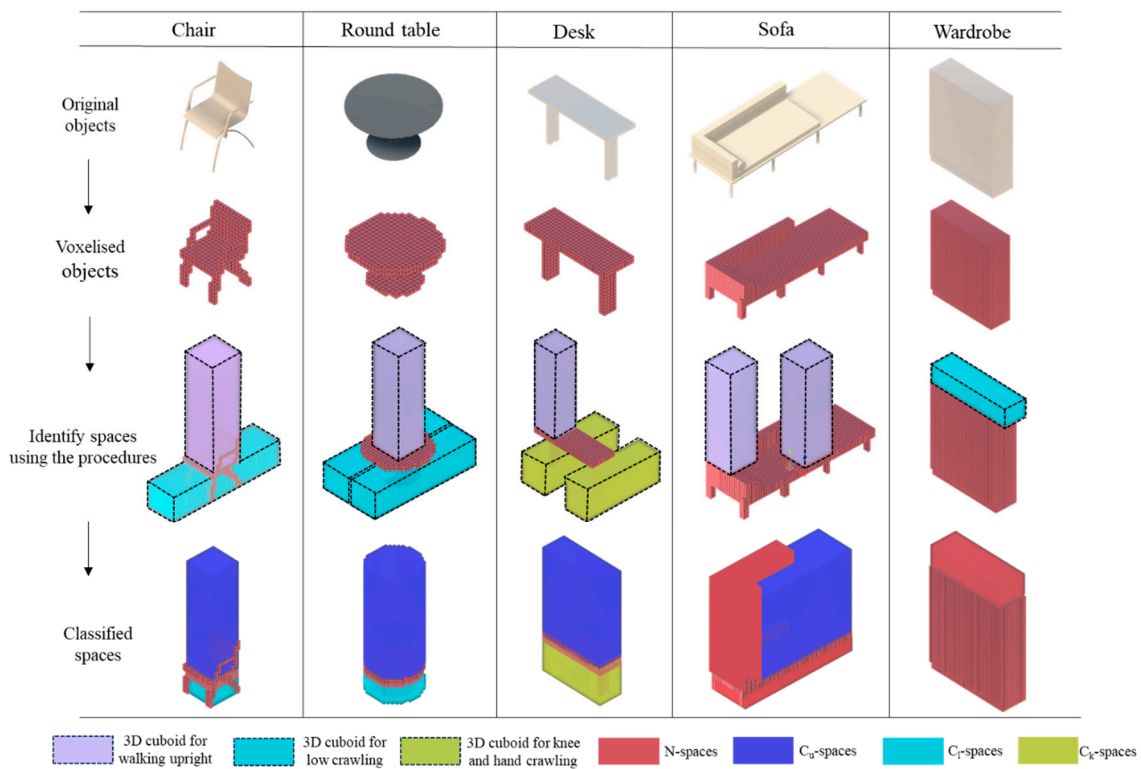


Figure 11. Identification and classification process of space components.

The spaces of the 3D indoor model are identified and classified into P-spaces, C_u -spaces, C_k -spaces, C_l -spaces and N-spaces with the five colours (green, blue, yellow, cyan and red). The openings of doors are regarded as P-spaces, while that of windows correspond to N-spaces. In simulations, windows are not usually allowed for pedestrian evacuations. Figure 12 shows the complete classification results of the 3D indoor model. For example, in the model, the spaces with a blue colour on the table and chair are used for walking upright, but the spaces with cyan are used for low crawling. Because this room has a higher ceiling, spaces above the movable objects are all used for walking upright.

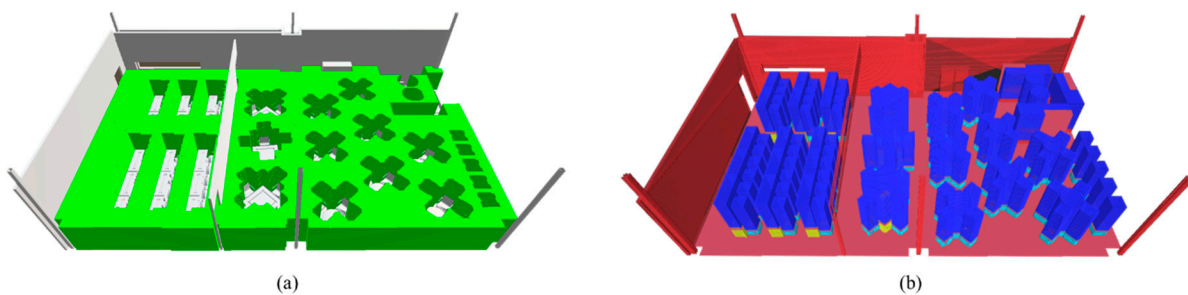


Figure 12. Three-dimensional voxel model of the furnished room with identified and classified space components: (a) P-spaces (green voxels), (b) C_u -spaces (blue voxels), C_k -spaces (yellow voxels), C_l -spaces (cyan voxels) and N-spaces (red voxels).

Let us suppose that in an emergency evacuation scenario, an individual perceives an environmental risk and starts to evacuate from the room. Figure 13 illustrates three cases. Here, the choice of 3D pedestrian motions is motivated by crowds and time pressure. Crowds may obstruct the individual from moving faster in high-density situations, so the individual might change the current movement and path to avoid being obstructed. In addition, due to time pressure, a faster movement might be chosen to evacuate from the indoor environment as soon as possible.

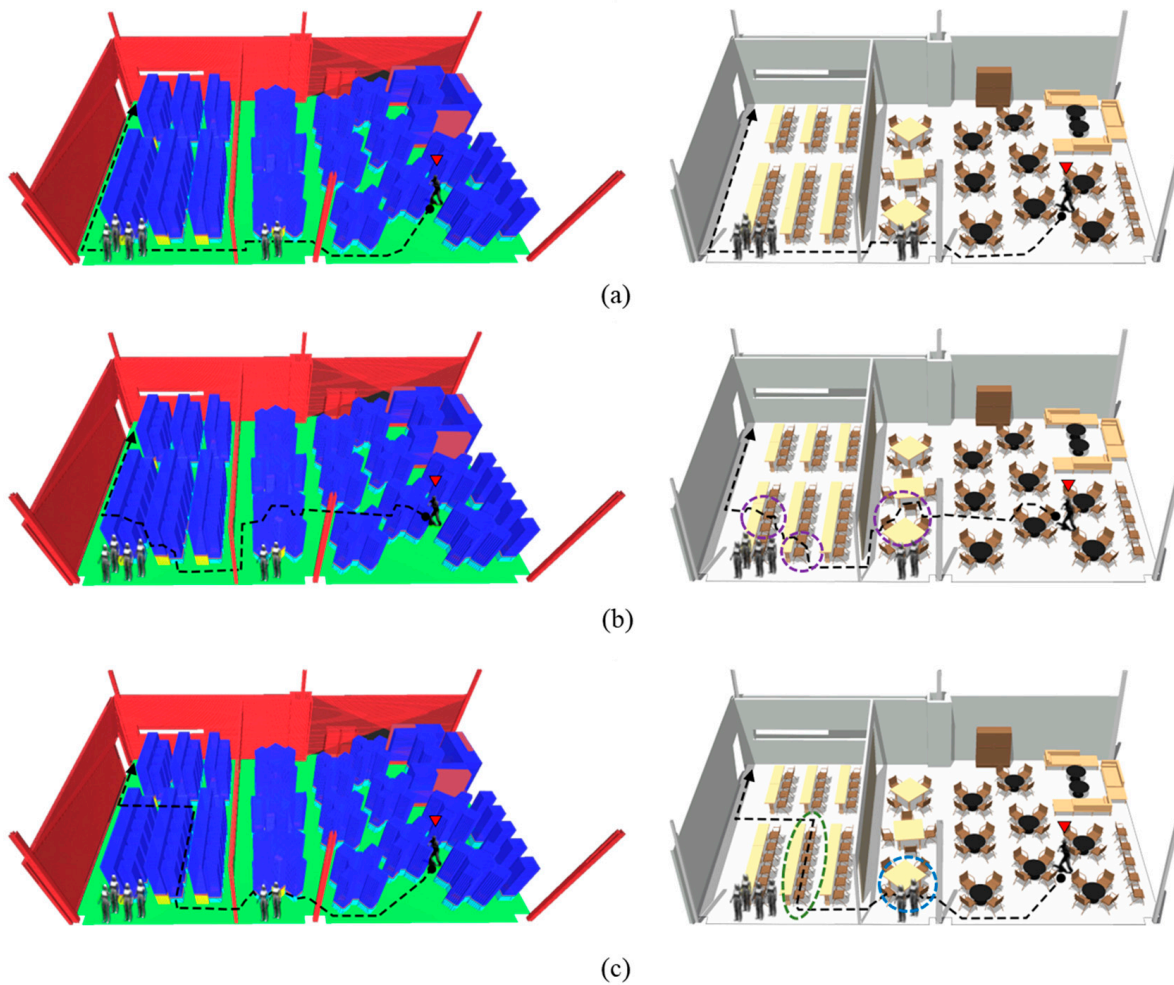


Figure 13. Diagram of evacuation paths in the furniture room. (a) A 2D path. (b) A 3D path using P-spaces and C_u -spaces. (c) A 3D path using P-spaces, C_k -spaces and C_l -spaces. N-spaces (red voxels), C-spaces (yellow and blue voxels) and P-spaces (green voxels).

In the first case (see Figure 13a), the 2D path relies on the P-spaces only, in which the individual has to bypass other pedestrians or wait in the queue for a while. Figure 13b shows a 3D evacuation path using C_u -spaces. A group of pedestrians obstructing the main evacuation path might cause the individual to move up/down the tables, desks and chairs, as highlighted by the purple round wireframes. The individual could adopt jumping up/down or climbing up/down to move through C_u -spaces above these objects. This might help the individual minimise speed changes to minimise his/her local evacuation time. In the third case (see Figure 13c), the individual might prefer low crawling and knee and hand crawling under chairs and desks for an evacuation path. The two movements do not require significant physical strength and ability. The green and blue round wireframes indicate the 3D path using C_k -spaces and C_l -spaces under chairs and desks. For an illustrative and clear visualisation purpose, C-spaces, N-spaces and the voxels of P-spaces neighbouring the floor slabs were set as visible. Note that we do not consider the effect of congestion on the individual around the width-fixed exit. The effect relates to the decision-making of exits, which requires special attention and is therefore outside the scope of this paper.

5. Conclusions and Future Work

This paper presented a conceptual space model, which can support simulating 3D pedestrian motions in indoor environments. We defined and characterised three space components for the motions: freely navigable spaces for pedestrians (P-spaces), navigable

spaces under conditions (C-spaces) and non-navigable spaces (N-spaces). C-spaces are further developed and classified into four types: C-spaces for low crawling (C_l -spaces), C-spaces for knee and hand crawling (C_k -spaces), C-spaces for bent-over walking (C_b -spaces) and C-spaces for walking upright (C_u -spaces). Finally, we employed a voxel-based approach to demonstrate the classification of the spaces in the conceptual model. This paper is deemed a starting point for providing a unified and flexible approach that addresses the limitation of existing 3D indoor models for 3D evacuation simulations, that is, spaces above/below physical components (e.g., tables, chairs, fences) in 3D space, which are navigable for pedestrians, are not fully identified and extracted.

The three types of space components have their unique attributes. P-spaces encompass the traditional walkable areas on floor slabs, stairs and ramps, enabling pedestrians to move without any additional hindrance. This classification is useful for simulating and understanding pedestrian movements in normal evacuations. By comparison, C-spaces introduce a novel dimension to indoor space classification. These spaces exist above or below physical components, allowing for 3D movements in exceptional circumstances. The sub-classification of C-spaces is particularly noteworthy, as it provides a detailed framework for understanding and simulating how pedestrians can behave in these complex 3D spaces, which facilitates addressing high emergency evacuation scenarios that require non-standard movement patterns, such as post-earthquakes, fires or terrorist attacks. Finally, N-spaces serve as a clear demarcation of where pedestrian motion is restricted or unreachable. Using P-, C- and N-spaces allows for more accurate modelling of pedestrian evacuation movement, especially in building scenes involving furniture or unique architectural features, such as teaching buildings, office buildings, opera houses, conference halls, libraries and nightclubs.

The representation of pedestrian shapes using 3D cuboids ensures consistency in describing different pedestrian movements, benefiting the simplicity, computational efficiency and flexibility of space classification. Specifically, the consistency of cuboids makes the space classification highly modular and adaptable. Its efficiency in a single room is expected to be highly scalable for larger scenarios, such as multi-room buildings or complexes. However, it is crucial to consider that while the model's core principles remain consistent, the computational load will invariably increase with scale. To address this, adjusting the cuboid sizes and voxel resolution to suit the scale of the environment becomes paramount in maintaining efficiency. In addition, a combination of various-sized cuboids to represent different body parts, such as the head, body and legs, could be a potential method to enhance the precision of the space classification. Nevertheless, this increased precision comes with a trade-off in terms of computational demand. Our decision to use a singular cuboid for a movement was driven by the need to balance accuracy with computational efficiency, ensuring that the model remains viable for large-scale scenarios. Users can adjust the size of the cuboids to adapt to the flexibility of pedestrian bodies according to their needs.

Moreover, 3D actions bridge the vertical gap between P-spaces and C-spaces, which empowers pedestrians to traverse changes in surface heights, expanding the capability of existing 3D indoor models beyond the conventional horizontal plane. A significant aspect of the 3D action is the use of a first-person perspective to describe the above/below positions of a pedestrian and surrounding physical components. The perspective aligns closely with the individual interactions with the environment, which benefits simulating the interactions in 3D space at a micro level. On the other hand, a third-person perspective that this paper does not explore provides a macro analysis view. It enables identifying bottlenecks, understanding pedestrian flows and observing patterns that might not be visible from a first-person perspective. We will further consider incorporating the third-person perspective in our evacuation simulation framework in future research.

Technically, the voxel-based approach could offer an efficient and comprehensive means of identifying and classifying space components. This approach addresses the inherent challenges of representing diverse 3D shapes and sizes of indoor spaces in traditional vector geometric models. Indeed, disasters like earthquakes or fires may change

the physical components and influence indoor space. For example, earthquakes can cause falling walls and ceilings. Even so, these potential environmental changes do not affect the effectiveness of the voxel-based approach. However, this requires investigating and synthesising temporal 3D geometry to model the changes in indoor space over time [1], which can be performed by establishing a database to store the update of the model in time series. On the other hand, some disasters influence pedestrian motion in direct ways. For instance, pedestrians tend to crawl in a fire to avoid smoke. These effects are more related to the interactions between disasters and pedestrians rather than indoor spaces, which are solved by simulating these disasters and the interactions. Some studies [46,52] have been devoted to the field.

Overall, our main future work will concentrate on further elaboration and testing of the current work as follows:

- Identifying how spaces may vary in size and distribution if different 3D cuboids are tailored to different pedestrian groups (e.g., kids, the aged).
- Determining how various height-related 3D actions effectively connect space components and the different thresholds of various height-related 3D actions.
- Investigating more details in methods/algorithms to classify indoor spaces automatically, especially different types of C-spaces.
- Investigating how the classified spaces are used for 3D evacuation simulations. Whether evacuation paths derived from space components and their connections are based on graphs or voxels warrants thorough analysis and comparison.
- Identifying key factors useful to simulate 3D pedestrian motions and establishing a 3D evacuation simulation model to simulate the motions, for example, simulating how different pedestrians decide to choose different motions and utilise different motions to adjust evacuation routes, etc.

Author Contributions: Conceptualisation, Ruihang Xie, Sisi Zlatanova and Jinwoo (Brian) Lee; Data Curation, Ruihang Xie; Formal Analysis, Ruihang Xie and Sisi Zlatanova; Investigation, Ruihang Xie and Sisi Zlatanova; Methodology, Ruihang Xie, Sisi Zlatanova and Mitko Aleksandrov; Resources, Ruihang Xie and Sisi Zlatanova; Software, Ruihang Xie and Mitko Aleksandrov; Supervision, Sisi Zlatanova and Jinwoo (Brian) Lee; Validation, Ruihang Xie and Sisi Zlatanova; Visualisation, Ruihang Xie; Writing—Original Draft, Ruihang Xie; Writing—Review and Editing, Sisi Zlatanova. All authors have read and agreed to the published version of the manuscript.

Funding: This research received no external funding.

Data Availability Statement: Data are contained within the article.

Acknowledgments: This research is supported by the University International Postgraduate Award from the University of New South Wales.

Conflicts of Interest: The authors declare no conflict of interest.

References

1. Xie, R.; Zlatanova, S.; Lee, J. 3D indoor environments in pedestrian evacuation simulations. *Automat. Constr.* **2022**, *144*, 104593. [[CrossRef](#)]
2. Haghani, M.; Sarvi, M. Simulating dynamics of adaptive exit-choice changing in crowd evacuations: Model implementation and behavioural interpretations. *Transp. Res. Part C Emerg. Technol.* **2019**, *103*, 56–82. [[CrossRef](#)]
3. Wang, X.; Mohcine, C.; Chen, J.; Li, R.; Ma, J. Modeling boundedly rational route choice in crowd evacuation processes. *Saf. Sci.* **2022**, *147*, 105590. [[CrossRef](#)]
4. Feliciani, C.; Murakami, H.; Shimura, K.; Nishinari, K. Efficiently informing crowds—Experiments and simulations on route choice and decision making in pedestrian crowds with wheelchair users. *Transp. Res. Part C Emerg. Technol.* **2020**, *114*, 484–503. [[CrossRef](#)]
5. Fu, Z.; Jia, Q.; Chen, J.; Ma, J.; Han, K.; Luo, L. A fine discrete field cellular automaton for pedestrian dynamics integrating pedestrian heterogeneity, anisotropy, and time-dependent characteristics. *Transp. Res. Part C Emerg. Technol.* **2018**, *91*, 37–61. [[CrossRef](#)]
6. Chooramun, N.; Lawrence, P.J.; Galea, E.R. An agent-based evacuation model utilising hybrid space discretisation. *Saf. Sci.* **2012**, *50*, 1685–1694. [[CrossRef](#)]

7. Liu, Q.; Lu, L.; Zhang, Y.; Hu, M. Modeling the dynamics of pedestrian evacuation in a complex environment. *Phys. A Stat. Mech. Its Appl.* **2022**, *585*, 126426. [[CrossRef](#)]
8. Guo, N.; Ding, J.; Ding, Z.; Zhu, K.; Wu, C. Crawling evacuation from a room: Experiment and modeling. *J. Stat. Mech. Theory Exp.* **2021**, *2021*, 33415. [[CrossRef](#)]
9. Song, Y.; Liu, J.; Liu, Q. Dynamic decision-making process of evacuees during post-earthquake evacuation near an automatic flap barrier gate system: A broken windows perspective. *Sustainability* **2021**, *13*, 8771. [[CrossRef](#)]
10. Delcea, C.; Cofas, L.; Craciun, L.; Molanescu, A.G. An agent-based modeling approach to collaborative classrooms evacuation process. *Saf. Sci.* **2020**, *121*, 414–429. [[CrossRef](#)]
11. Xie, R.; Zlatanova, S.; Lee, J.B. 3D indoor-pedestrian interaction in emergencies: A review of actual evacuations and simulation models. *Int. Arch. Photogramm. Remote Sens. Spat. Inf. Sci.* **2022**, *XLVIII-4/W4-2022*, 183–190. [[CrossRef](#)]
12. Gorte, B.; Aleksandrov, M.; Zlatanova, S. Towards egress modelling in voxel building models. *ISPRS Ann. Photogramm. Remote Sens. Spat. Inf. Sci.* **2019**, *IV-4/W9*, 43–47. [[CrossRef](#)]
13. Aleksandrov, M.; Heslop, D.J.; Zlatanova, S. 3D indoor environment abstraction for crowd simulations in complex buildings. *Buildings* **2021**, *11*, 445. [[CrossRef](#)]
14. You, L.; Zhang, C.; Hu, J.; Zhang, Z. A three-dimensional cellular automata evacuation model with dynamic variation of the exit width. *J. Appl. Phys.* **2014**, *115*, 224905. [[CrossRef](#)]
15. Wei, J.; Zhang, H.; Guo, Y.; Gu, M. Experiment of bi-direction pedestrian flow with three-dimensional cellular automata. *Phys. Lett. A* **2015**, *379*, 1081–1086. [[CrossRef](#)]
16. Jun, H.; Huijun, S.; Juan, W.; Xiaodan, C.; Lei, Y.; Musong, G. Experiment and modeling of paired effect on evacuation from a three-dimensional space. *Phys. Lett. A* **2014**, *378*, 3419–3425. [[CrossRef](#)]
17. Bandi, S.; Thalmann, D. Space discretization for efficient human navigation. *Comput. Graph. Forum* **1998**, *17*, 195–206. [[CrossRef](#)]
18. Li, F.; Zlatanova, S.; Koopman, M.; Bai, X.; Diakit , A. Universal path planning for an indoor drone. *Automat. Constr.* **2018**, *95*, 275–283. [[CrossRef](#)]
19. Han, B.; Qu, T.; Tong, X.; Jiang, J.; Zlatanova, S.; Wang, H.; Cheng, C. Grid-optimized UAV indoor path planning algorithms in a complex environment. *Int. J. Appl. Earth Obs.* **2022**, *111*, 102857. [[CrossRef](#)]
20. Beno, P.; Pavelka, V.; Duchon, F.; Dekan, M. Using octree maps and RGBD cameras to perform mapping and a navigation. In Proceedings of the 2016 International Conference on Intelligent Networking and Collaborative Systems (INCoS), Ostrava, Czech Republic, 7–9 September 2016; pp. 66–72. [[CrossRef](#)]
21. Zhao, J.; Xu, Q.; Zlatanova, S.; Liu, L.; Ye, C.; Feng, T. Weighted octree-based 3D indoor pathfinding for multiple locomotion types. *Int. J. Appl. Earth Obs.* **2022**, *112*, 102900. [[CrossRef](#)]
22. Rodenberg, O.; Verbree, E.; Zlatanova, S. Indoor A* pathfinding through an octree representation of a point cloud. *ISPRS Ann. Photogramm. Remote Sens. Spat. Inf. Sci.* **2016**, *4*, 249–255. [[CrossRef](#)]
23. Fichtner, F.W.; Diakit , A.A.; Zlatanova, S.; Vo te, R. Semantic enrichment of octree structured point clouds for multi-story 3D pathfinding. *Trans. GIS* **2018**, *22*, 233–248. [[CrossRef](#)]
24. Zlatanova, S.; Liu, L.; Sithole, G.; Zhao, J.; Mortari, F. Space subdivision for indoor applications. *GIST Rep. No. 66* **2014**. Available online: <http://resolver.tudelft.nl/uuid:c3ef4c87-9c35-4d05-8877-a074c3f7fdbf> (accessed on 19 November 2021).
25. Wang, Q.; Song, W.; Zhang, J.; Ye, R.; Ma, J. Experimental study on knee and hand crawling evacuation for different age group students. *Int. J. Disaster Risk Reduct.* **2020**, *48*, 101613. [[CrossRef](#)]
26. Jia, X.; Feliciani, C.; Yanagisawa, D.; Nishinari, K. Experimental study on the evading behavior of individual pedestrians when confronting with an obstacle in a corridor. *Phys. A Stat. Mech. Its Appl.* **2019**, *531*, 121735. [[CrossRef](#)]
27. Nagai, R.; Fukamachi, M.; Nagatani, T. Evacuation of crawlers and walkers from corridor through an exit. *Phys. A Stat. Mech. Its Appl.* **2006**, *367*, 449–460. [[CrossRef](#)]
28. Kady, R.A.; Davis, J. The effect of occupant characteristics on crawling speed in evacuation. *Fire Saf. J.* **2009**, *44*, 451–457. [[CrossRef](#)]
29. Kady, R.A.; Davis, J. The impact of exit route designs on evacuation time for crawling occupants. *J. Fire Sci.* **2009**, *27*, 481–493. [[CrossRef](#)]
30. Gallagher, S.; Pollard, J.; Porter, W.L. Locomotion in restricted space: Kinematic and electromyographic analysis of stoopwalking and crawling. *Gait Posture* **2011**, *33*, 71–76. [[CrossRef](#)]
31. Davis, J.; Gallagher, S. Physiological demand on firefighters crawling during a search exercise. *Int. J. Ind. Ergonom.* **2014**, *44*, 821–826. [[CrossRef](#)]
32. Cao, L.; Davis, G.A.; Gallagher, S.; Schall, M.C.; Sesek, R.F. Characterizing posture and associated physiological demand during evacuation. *Saf. Sci.* **2018**, *104*, 1–9. [[CrossRef](#)]
33. Ma, J.; Shi, D.; Li, T.; Li, X.; Xu, T.; Lin, P. Experimental study of single-file pedestrian movement with height constraints. *J. Stat. Mech. Theory Exp.* **2020**, *2020*, 73409. [[CrossRef](#)]
34. Ding, Z.; Shen, Z.; Guo, N.; Zhu, K.; Long, J. Evacuation through area with obstacle that can be stepped over: Experimental study. *J. Stat. Mech.* **2020**, *2020*, 23404. [[CrossRef](#)]
35. Thompson, P.A. Developing New Techniques for Modelling Crowd Movement. KB Thesis Scanning Project 2015. Ph.D. Thesis, University of Edinburgh, Edinburgh, UK, 1994.

36. Waş, J.; Gudowski, B.; Matuszyk, P.J. Social distances model of pedestrian dynamics. In Proceedings of the Cellular Automata: 7th International Conference on Cellular Automata, for Research and Industry, ACRI 2006, Perpignan, France, 20–23 September 2006; Proceedings 7. pp. 492–501. [\[CrossRef\]](#)
37. Waş, J.; Lubaś, R. Adapting Social Distances Model for Mass Evacuation Simulation. *J. Cell. Autom.* **2013**, *8*, 395–405.
38. Chraïbi, M.; Seyfried, A.; Schadschneider, A. Generalized centrifugal-force model for pedestrian dynamics. *Phys. Rev. E* **2010**, *82*, 46111. [\[CrossRef\]](#)
39. Li, M.; Zhao, Y.; He, L.; Chen, W.; Xu, X. The parameter calibration and optimization of social force model for the real-life 2013 Ya’an earthquake evacuation in China. *Saf. Sci.* **2015**, *79*, 243–253. [\[CrossRef\]](#)
40. Alonso-Marroquín, F.; Busch, J.; Ramírez-Gómez, Á.; Lozano, C. A discrete spheropolygon model for calculation of stress in crowd dynamics. In *Traffic and Granular Flow’13*; Springer: Cham, Switzerland, 2015; pp. 179–186. [\[CrossRef\]](#)
41. Alonso-Marroquín, F.; Busch, J.; Chiew, C.; Lozano, C.; Ramírez-Gómez, Á. Simulation of counterflow pedestrian dynamics using spheropolygons. *Phys. Rev. E* **2014**, *90*, 63305. [\[CrossRef\]](#)
42. Chraïbi, M.; Kemloh, U.; Schadschneider, A.; Seyfried, A. Force-based models of pedestrian dynamics. *Netw. Heterog. Media* **2011**, *6*, 425. [\[CrossRef\]](#)
43. Hidalgo, R.C.; Parisi, D.R.; Zuriguel, I. Simulating competitive egress of noncircular pedestrians. *Phys. Rev. E* **2017**, *95*, 42319. [\[CrossRef\]](#)
44. Wang, K.; Fu, Z.; Li, Y.; Qian, S. Influence of human-obstacle interaction on evacuation from classrooms. *Automat. Constr.* **2020**, *116*, 103234. [\[CrossRef\]](#)
45. Maniccam, S. Traffic jamming on hexagonal lattice. *Phys. A Stat. Mech. Its Appl.* **2003**, *321*, 653–664. [\[CrossRef\]](#)
46. Zheng, Y.; Jia, B.; Li, X.; Jiang, R. Evacuation dynamics considering pedestrians’ movement behavior change with fire and smoke spreading. *Saf. Sci.* **2017**, *92*, 180–189. [\[CrossRef\]](#)
47. Yakhou, N.; Thompson, P.; Siddiqui, A.; Abualdenien, J.; Ronchi, E. The integration of building information modelling and fire evacuation models. *J. Build. Eng.* **2023**, *63*, 105557. [\[CrossRef\]](#)
48. Król, A.; Król, M. Numerical investigation on fire accident and evacuation in a urban tunnel for different traffic conditions. *Tunn. Undergr. Sp. Tech.* **2021**, *109*, 103751. [\[CrossRef\]](#)
49. Huang, Y.; Guo, Z.; Chu, H.; Sengupta, R. Evacuation Simulation Implemented by ABM-BIM of Unity in Students’ Dormitory Based on Delay Time. *ISPRS Int. J. Geo-Inf.* **2023**, *12*, 160. [\[CrossRef\]](#)
50. Unity Technologies. Unity User Manual 2020.3 (LTS). Available online: <https://docs.unity3d.com/Manual/index.html> (accessed on 21 December 2021).
51. Thunderhead Engineering. Pathfinder Technical Reference Manual. Available online: <https://support.thunderheadeng.com/docs/pathfinder/2021-4/technical-reference-manual/> (accessed on 21 December 2021).
52. Chen, J.; Shi, T.; Li, N. Pedestrian evacuation simulation in indoor emergency situations: Approaches, models and tools. *Saf. Sci.* **2021**, *142*, 105378. [\[CrossRef\]](#)
53. Lee, J.; Li, K.-J.; Zlatanova, S.; Kolbe, T.H.; Nagel, C.; Becker, T. Open Geospatial Consortium IndoorGML v. 1.0, OGC. Available online: <https://docs.ogc.org/is/14-005r3/14-005r3.html> (accessed on 2 June 2014).
54. Kolbe, T.H.; Kutzner, T.; Smyth, C.S.; Nagel, C.; Roensdorf, C.; Heazel, C. Open Geospatial Consortium CityGML. Available online: <https://docs.ogc.org/guides/20-066.html> (accessed on 19 May 2022).
55. Boguslawski, P.; Gold, C.M.; Ledoux, H. Modelling and analysing 3D buildings with a primal/dual data structure. *ISPRS J. Photogramm.* **2011**, *66*, 188–197. [\[CrossRef\]](#)
56. Zlatanova, S.; Liu, L.; Sithole, G. A conceptual framework of space subdivision for indoor navigation. In Proceedings of the fifth ACM SIGSPATIAL International Workshop on Indoor Spatial Awareness, Orlando, FL, USA, 5 November 2013; pp. 37–41. [\[CrossRef\]](#)
57. Mortari, F.; Clementini, E.; Zlatanova, S.; Liu, L. An indoor navigation model and its network extraction. *Appl. Geomat.* **2019**, *11*, 413–427. [\[CrossRef\]](#)
58. Kr, U.; Minaitundefined, M.; Zlatanova, S. Indoor space subdivision for indoor navigation. In *ISA ’14*; ACM: New York, NY, USA, 2014; pp. 25–31. [\[CrossRef\]](#)
59. Zlatanova, S.; Yan, J.; Wang, Y.; Diakit , A.; Isikdag, U.; Sithole, G.; Barton, J. Spaces in spatial science and urban applications—State of the Art Review. *ISPRS Int. J. Geo-Inf.* **2020**, *9*, 58. [\[CrossRef\]](#)
60. Richter, K.; Winter, S.; R etschi, U. Constructing hierarchical representations of indoor spaces. In Proceedings of the 2009 Tenth International Conference on Mobile Data Management: Systems, Services and Middleware, Taipei, Taiwan, 18–20 May 2009; pp. 686–691. [\[CrossRef\]](#)
61. Yan, J.; Diakit , A.A.; Zlatanova, S. A generic space definition framework to support seamless indoor/outdoor navigation systems. *Trans. GIS* **2019**, *23*, 1273–1295. [\[CrossRef\]](#)
62. Diakit , A.A.; Zlatanova, S. Spatial subdivision of complex indoor environments for 3D indoor navigation. *Int. J. Geogr. Inf. Sci.* **2018**, *32*, 213–235. [\[CrossRef\]](#)
63. Nikoohemat, S.; Diakit , A.A.; Zlatanova, S.; Vosselman, G. Indoor 3D reconstruction from point clouds for optimal routing in complex buildings to support disaster management. *Automat. Constr.* **2020**, *113*, 103109. [\[CrossRef\]](#)
64. Claridades, A.R.C.; Choi, H.; Lee, J. An indoor space subsampling framework for implementing a 3d hierarchical network-based topological data model. *ISPRS Int. J. Geo-Inf.* **2022**, *11*, 76. [\[CrossRef\]](#)

65. Sithole, G.; Zlatanova, S. Position, location, place and area: An indoor perspective. *ISPRS Ann. Photogramm. Remote Sens. Spat. Inf. Sci* **2016**, *3*, 89–96. [[CrossRef](#)]
66. Gorte, B. Analysis of very large voxel datasets. *Int. J. Appl. Earth Obs.* **2023**, *119*, 103316. [[CrossRef](#)]
67. Liu, L.; Li, B.; Zlatanova, S.; van Oosterom, P. Indoor navigation supported by the Industry Foundation Classes (IFC): A survey. *Automat. Constr.* **2021**, *121*, 103436. [[CrossRef](#)]

Disclaimer/Publisher’s Note: The statements, opinions and data contained in all publications are solely those of the individual author(s) and contributor(s) and not of MDPI and/or the editor(s). MDPI and/or the editor(s) disclaim responsibility for any injury to people or property resulting from any ideas, methods, instructions or products referred to in the content.